Title

Itaconate modulates tricarboxylic acid and redox metabolism to mitigate reperfusion injury.

Authors

Cordes, Thekla
Lucas, Alfredo
Divakaruni, Ajit S
et al.

Publication Date

2020-02-01

DOI

10.1016/j.molmet.2019.11.019

Peer reviewed

Original Article

MOLECULAR METABOLISM

Itaconate modulates tricarboxylic acid and redox metabolism to mitigate reperfusion injury

Thekla Cordes [1], Alfredo Lucas [1], Ajit S. Divakaruni [2,3], Anne N. Murphy [2], Pedro Cabrales [1], Christian M. Metallo [1,*]

ABSTRACT

Objectives: Cerebral ischemia/reperfusion (IR) drives oxidative stress and injurious metabolic processes that lead to redox imbalance, inflammation, and tissue damage. However, the key mediators of reperfusion injury remain unclear, and therefore, there is considerable interest in therapeutically targeting metabolism and the cellular response to oxidative stress.

Methods: The objective of this study was to investigate the molecular, metabolic, and physiological impact of itaconate treatment to mitigate reperfusion injuries in in vitro and in vivo model systems. We conducted metabolic flux and bioenergetic studies in response to exogenous itaconate treatment in cultures of primary rat cortical neurons and astrocytes. In addition, we administered itaconate to mouse models of cerebral reperfusion injury with ischemia or traumatic brain injury followed by hemorrhagic shock resuscitation. We quantitatively characterized the metabolite levels, neurological behavior, markers of redox stress, leukocyte adhesion, arterial blood flow, and arteriolar diameter in the brains of the treated/untreated mice.

Results: We demonstrate that the "immunometabolite" itaconate slowed tricarboxylic acid (TCA) cycle metabolism and buffered redox imbalance via succinate dehydrogenase (SDH) inhibition and induction of anti-oxidative stress response in primary cultures of astrocytes and neurons. The addition of itaconate to reperfusion fluids after mouse cerebral IR injury increased glutathione levels and reduced reactive oxygen/nitrogen species (ROS/RNS) to improve neurological function. Plasma organic acids increased post-reperfusion injury, while administration of itaconate normalized these metabolites. In mouse cranial window models, itaconate significantly improved hemodynamics while reducing leukocyte adhesion. Further, itaconate supplementation increased survival in mice experiencing traumatic brain injury (TBI) and hemorrhagic shock.

Conclusions: We hypothesize that itaconate transiently inhibits SDH to gradually "awaken" mitochondrial function upon reperfusion that minimizes ROS and tissue damage. Collectively, our data indicate that itaconate acts as a mitochondrial regulator that controls redox metabolism to improve physiological outcomes associated with IR injury.

Keywords Itaconate; Succinate dehydrogenase (SDH); Cerebral ischemia/reperfusion (IR); Redox stress; Mitochondrial metabolism; Brain injury

1. INTRODUCTION

Brain damage and cerebral ischemic insults such as stroke and traumatic brain injuries (TBI) limit oxygen and nutrient supplies to the brain, which results in massive redox imbalance, tissue damage, neuronal death, and irreversible neurological consequences. While reperfusion is necessary for survival, it is associated with the induction of oxidative stress and inflammatory responses in cells that survive the initial ischemic insult [1,2]. These latter events markedly exacerbate the initial depletion of oxygen and nutrients via metabolic reprogramming, production of reactive oxygen and nitrogen species (ROS and RNS), and induction of inflammatory signals [3–6]. However, effective therapies to address key mediators of reperfusion injury remain elusive. De-energization results in the loss of ionic homeostasis that, in turn, triggers the cascade of ischemia/reperfusion (IR) injury and inability of cellular organelles, specifically mitochondria, to re-establish normal metabolic function that is a primary determinant of tissue survival [7–9]. Ultimately, reperfusion injury can drive extensive tissue damage and increase the risk of sepsis and multiple organ failure [10–12]. As a significant unmet medical need, there is current interest in therapeutically targeting metabolism to improve outcomes [13,14].

[1]Department of Bioengineering, University of California, San Diego, 9500 Gilman Drive, 92093 La Jolla, CA, USA [2]Department of Pharmacology, University of California, San Diego, 9500 Gilman Drive, 92093 La Jolla, CA, USA

[3] Current address: Department of Molecular and Medical Pharmacology, University of California, 90095 Los Angeles, Los Angeles, CA, USA.

*Corresponding author. E-mail: cmetallo@ucsd.edu (C.M. Metallo).

Received October 2, 2019 • Revision received November 25, 2019 • Accepted November 29, 2019 • Available online 13 December 2019

https://doi.org/10.1016/j.molmet.2019.11.019

Abbreviations

[U−^{13}C]substrate	Uniformly labeled ^{13}C carbon tracer
CAD/IRG1	Cis-aconitate decarboxylase/immunoresponsive gene 1 protein
ATF3	Activating transcription factor 3
CCA	Common carotid arteries
CSF	Cerebrospinal fluid
DHR-123	Dihydrorhodamine-123
DMM	Dimethyl malonate
G6pd	Glucose-6-phosphate dehydrogenase
Gclm	Glutamate-cysteine ligase
Gpx1	Glutathione peroxidase 1
GSH	Reduced glutathione
Gsr	Glutathione reductase
GSSG	Oxidized glutathione
Hmox1	Heme oxygenase 1
HS	Hemorrhagic shock
IR	Ischemia/reperfusion
KEAP1	Kelch-like ECH-associated protein 1
LR	Lactated Ringer's solution
MAP	Mean arterial pressure
MCA	Middle cerebral artery
NMDA	N-methyl-D-aspartate
NO	Nitric oxide
NOS	Nitric oxide synthase
Nqo1	NAD(P)H dehydrogenase
Nrf2	Nuclear factor erythroid 2-related factor 2
PMP	Plasma membrane permeabilizer
RET	Reverse electron transport
RNS	Reactive nitrogen species
ROS	Reactive oxygen species
SDH	Succinate dehydrogenase
TCA	Tricarboxylic acid
TBI	Traumatic brain injury

Although direct antioxidants have failed clinically [15], therapies to improve survival and recovery from IR injury, such as cerebral ischemia, stroke, and TBI, must directly or indirectly reduce oxidative stress, which is characterized by an imbalance between ROS generation and anti-oxidant defense systems. Succinate dehydrogenase (SDH) activity drives a significant portion of ROS generation, and it has been demonstrated that SDH inhibition by malonate is protective against reperfusion injuries [5]. Notably, itaconate inhibits SDH in a dose-dependent manner, leading to succinate accumulation [16,17]. Itaconate is synthesized de novo in myeloid cells by decarboxylation of the tricarboxylic acid (TCA) cycle intermediate cis-aconitate via the enzyme cis-aconitate decarboxylase/immunoresponsive gene 1 protein (CAD/IRG1), which is highly expressed under pro-inflammatory conditions [18–21]. Although macrophages produce endogenous itaconate at mM levels [16,18,22], this metabolite is secreted at low rates and is not detectable at high concentrations in humans with acute inflammation or sepsis [23]. We therefore hypothesized that itaconate could serve as a stable degradable inhibitor of SDH to attenuate ROS production from the electron transport chain during reperfusion.

In addition, an anti-inflammatory role for synthetic cell-permeable derivatives of itaconate has been described, where itaconyl esters alkylate cysteine residues on the Kelch-like ECH-associated protein 1 (KEAP1), enabling stabilization of nuclear factor erythroid 2-related factor 2 (Nrf2) and also induce activating transcription factor 3 (ATF3)-dependent pathways [24,25]. Importantly, Nrf2 activation induces the expression of ROS scavenging enzymes, anti-inflammatory, and cytoprotective genes that limit oxidative damage triggered by ischemia and brain injury [26,27].

Little is known about the impact of exogenous itaconate on metabolism, redox stress, and ischemic damage. In this study, we investigated the metabolic and physiological effects of itaconate treatment in cultured cortical neurons and astrocytes as well as on mouse models of cerebral reperfusion injury. We hypothesize that the administration of itaconate preserves metabolic function, thereby reducing cellular damage upon ischemic insults. Specifically, we observed that itaconate treatment inhibits SDH and promotes gene expression associated with anti-oxidant pathways. When administered prior to reperfusion in mouse models of cerebral ischemia and TBI with hemorrhagic shock (HS), itaconate reduced oxidative stress and improved cerebral hemodynamics, inflammation, neurological function, and survival. These results provide evidence that itaconate mitigates pathology associated with reperfusion injury.

2. MATERIALS AND METHODS

2.1. Study approval

Animal handling and care was approved by the Institutional Animal Care and Use Committee of the University of California, San Diego, CA, and was conducted accordingly to the Guide for the Care and Use of Laboratory Animals (US National Research Council, 2010). C57BL/6J mice were obtained from Jackson Laboratories (Bar Harbor, ME, USA).

2.2. Animal model of cerebral ischemia reperfusion

Acute cerebral ischemia was achieved by placing two micro clips in tandem on the left middle cerebral artery (MCA) at 1 mm proximal to the MCA bifurcation but distal to the origin of the lenticulostriate arteries. This was immediately followed by the ligation of the bilateral common carotid arteries (CCA). For occlusion reperfusion, the clips and CCA ligations were removed 60 min after the start of occlusion, respectively. During the experiment, both brain and rectal temperatures were maintained at approximately 37 °C with an external heating pad. Temperatures and blood pressure were continuously monitored. Arterial blood gases were examined at pre-occlusion and 120 min after the start of occlusion. Itaconate was infused for 30 min at 15 mg/kg/min prior to ligation, stopped during ligation, and infused again for 30 min during reperfusion. Itaconate was dissolved in 0.9% NaCl solution (Hospira Inc.) and adjusted to pH = 7.2. A vehicle group was infused with 0.9% NaCl. A sham group underwent surgery but without ligation. Male mice aged nine weeks were used to study ischemia reperfusion.

2.3. Animal model of traumatic brain injury (TBI) followed by hemorrhagic shock (HS)

The mice were subjected to fluid percussion TBI followed by hemorrhage of 50% of the animal's blood volume. Thirty min after the trauma, volume fluid resuscitation was accomplished according to the Tactical Combat Casualty Care (TCCC) field care guidelines, preserving the mean arterial pressure (MAP) above 70 mmHg for 4 h. Fluid resuscitation was accomplished using lactated Ringer's solution (LR), Hextend (6% Hetastarch in Lactated Electrolyte Injection, Hospira Inc., Lake Forest, IL, USA), or Hextend with 15 mg/mL of itaconate. The

itaconate solution was adjusted to pH = 7.2. After 4 h, the mice were placed in their cages with free access to food and water for 7 days (all groups with n = 6). The mean arterial blood pressure (MAP) was measured on a temperature-controlled platform. Male mice aged nine weeks were used to study TBI/HS.

2.4. Glutathione measurements

Total glutathione as well as reduced (GSH) and oxidized glutathione (GSSG) in the brain tissue were measured using enzyme-linked assay kits (Cayman Chemical, Ann Arbor, MI, USA). The brain was removed, weighed and one of the hemispheres was processed for the measurement of total glutathione (GSH + GSSG) and GSSG. The brain sample was homogenized in 5 mL of cold buffer per gram of tissue using a T25 basic electric homogenizer. The precipitate was removed by centrifugation and the supernatant was collected and frozen until assaying.

2.5. Neurological function (motor score)

After the ischemic insult, the mice were subjected to a series of neurologic tests designed to detect motor deficits [28]. Briefly, the mice were placed on a rotating 15 × 15 cm screen (grid size 0.2 × 0.2 cm). The duration of time that the mouse could hold onto the screen after it was rotated from horizontal to vertical was recorded. Next, the amount of time that the mouse could remain balanced on a horizontal board was recorded. Finally, the mouse underwent a prehensile traction test by timing up to 5 s the period that the mouse could cling to a horizontal rope. Using these three tests, a maximal score of 25 and a minimal score of 0 was obtained.

2.6. Cerebral reactive oxygen/nitrogen species (ROS/RNS)

Oxidant-sensitive dihydrorhodamine-123 (DHR-123, Molecular Probes Inc., 20 μmol/L) was used to quantify the oxidant production in the cerebral venules following ischemia reperfusion [29]. Briefly, the DHR-123 was dissolved in artificial cerebrospinal fluid (CSF) and super fused on the brain surface of the closed cranial window. The brain tissue was exposed to the DHR for 15 min, followed by suffusion with plain artificial CSF. DHR oxidation was visualized and quantified. DHR fluorescence intensity was monitored in a region of the brain surface that was equivalent to twice the area of the venular segment under study and in a rectangular area immediately outside the vessels.

2.7. Mice cranial window model

The closed cranial window model was implanted in mice anesthetized with ketamine-xylazine. The mice were first administered dexamethasone (0.2 mg/kg), carprofen (5 mg/kg), and ampicillin (6 mg/kg) subcutaneously to prevent swelling of the brain, inflammatory response, and infection. After shaving the head and cleansing with ethanol 70% and betadine, the mouse was placed on a stereotaxic frame and the head immobilized using ear bars. The scalp was removed with sterilized surgical instruments, and lidocaine-epinephrine was applied on the periosteum, which was then retracted, exposing the skull. A 3- to 4-mm-diameter skull opening was made in the left parietal bone using a surgical drill. Under a saline drip, the craniotomy was lifted away from the skull with very thin tip forceps and Gelfoam previously soaked in saline was applied to the dura mater to stop any eventual minor bleeding. The exposed area was covered with a 5 mm glass coverslip secured with cyanoacrylate-based glue and dental acrylic. Carprofen and ampicillin were administered daily for three to five days after recovery from surgery. One week after surgery, the mice were lightly anesthetized with isoflurane to complete the ischemic model. A panoramic picture of the vessels under the window was taken, and then mice were transferred to an intravital microscope stage (customized Leica-McBain, San Diego, CA, USA). Body temperature was maintained using a heating pad. Using water-immersion objectives (× 20), blood vessel images were captured (Cohu 4815, Cohu, Inc., San Diego, CA, USA) and recorded on videotape. An image shear device (Image Shear, Vista Electronics, San Diego, CA, USA) was used to measure the baseline vessel diameters (D), and the RBC velocities (V) were measured offline by cross-correlation (Photo Diode/Velocity Tracker Model 102B, Vista Electronics, San Diego, CA, USA). Measurements of the pial arterioles (diameter range: <20 μm (small vessels), 21–50 μm (medium vessels), and 51–100 μm (large vessels), each n = 14–15) were performed in each animal, and the blood flow (Q) in each individual vessel was calculated using the equation: $Q = V \times \pi(D/2)^2$. Adherent and rolling leukocytes were visualized by anti-CD45-TxR antibodies (Caltag, Carlsbad, CA, USA) and infused via i.v. Green fluorescence (518 nm) emitted by albumin-FITC and GFP (PbA-GFP pRBC) was captured using ALPHA Vivid: XF100-2 (Omega Optical, Brattleboro, VT, USA), and anti-CD45-TxR fluorescence (615 nm) was exited and captured with a Vivid Standard XF42.

2.8. Primary cortical neurons and astrocytes

Primary cortical neurons and astrocytes were generated from embryonic day 18 Sprague–Dawley rats as previously described [30,31]. Briefly, cortical neurons were plated onto poly-D-lysine-coated wells of 96-well Seahorse XFe96 plates (2.5×10^4 cells/well) or 12-well dishes (1×10^5 cells/well) and maintained at 37 °C in a humidified incubator with 5% CO_2. The cells were maintained in maintenance medium composed of neurobasal medium (Thermo Fisher Scientific) supplemented with 1 × B27 of serum-free supplement (Thermo Fisher Scientific), 2 mM of GlutaMAX (Thermo Fisher Scientific), 100 U/ml of penicillin, and 100 μg/ml of streptomycin. Half of the medium was replaced every 3–4 days. The experiments were conducted on day in vitro (DIV) 19–21. Cortical astrocytes were prepared according to [32] and plated onto 12-well culture plates (1×10^5 cells/well). Primary astrocytes were cultivated in DMEM (Sigma–Aldrich, D5030) supplemented with 10% FBS, 100 U/ml of penicillin, 100 μg/ml of streptomycin, 10 mM of glucose, and 0.5 mM of glutamine.

2.9. Isotopic tracing

For isotopic labeling experiments, primary neurons were cultured in custom Neuro-c medium as previously described in detail [31]. For tracing studies, ^{12}C glucose was replaced with 8 mM of [U–$^{13}C_6$] glucose (Cambridge Isotopes, CLM-1396), ^{12}C leucine was replaced with 0.8 mM of [U–$^{13}C_6$]leucine (Cambridge Isotopes, CLM2-2262), or 2 mM of [U–$^{13}C_4$]β-hydroxybutyrate (Sigma–Aldrich 606030) was supplemented to the medium. For tracing with labeled glutamine, GlutaMAX was omitted and replaced with 0.5 mM of [U–$^{13}C_5$]glutamine (Cambridge Isotopes, CLM-1822) and N-methyl-D-aspartate (NMDA) receptor antagonist MK801 (10 μM) was added to prevent excitotoxic neuronal injury. Primary astrocytes were cultured in DMEM medium (Sigma–Aldrich, D5030) containing 10 mM of glucose, 10% FBS, 100 U/ml of penicillin, 100 μg/ml of streptomycin, and 0.5 mM of [U–$^{13}C_5$] glutamine. The cells were cultured in medium containing stable isotope tracers of choice as indicated in the text. For itaconate degradation studies, primary cortical neurons were exposed to 2 mM and primary astrocytes to 1 mM of exogenous [U–$^{13}C_5$]itaconate for 48 h (NIH Metabolite Standards Synthesis Core). The cultured cells were exposed to 2 mM of exogenous itaconate (Sigma–Aldrich, Cat. No. I29204) as indicated in the text. All of the media were adjusted to pH = 7.3.

Mass isotopomer distributions and total metabolite abundances were computed by the integration of mass fragments using a MATLAB-based INCA algorithm with corrections for natural isotope abundances as previously described [33]. Labeling was depicted as the isotopologue distribution or ^{13}C incorporation into metabolite (mole percent enrichment) [34].

2.10. Gas chromatograph-mass spectrometry (GC—MS), sample preparation, and analysis

The metabolites were extracted, analyzed, and quantified as previously described in detail by Cordes and Metallo [34]. Briefly, the cells were washed with saline solution and quenched with 0.25 ml of −20 °C methanol. After adding 0.1 ml of 4 °C water, the cells were collected in tubes containing 0.25 ml of −20 °C chloroform. Plasma metabolites were extracted using 5 μl of plasma, 0.25 ml of −20 °C methanol, 0.1 ml of 4 °C cold water, and 0.25 ml of −20 °C chloroform. The extracts were vortexed for 10 min at 4 °C and centrifuged at 16,000× *g* for 5 min at 4 °C. The upper aqueous phase was evaporated under a vacuum at 4 °C. Derivatization for polar metabolites was performed using a Gerstel MPS with 15 μl of 2% (w/v) methoxyamine hydrochloride (Thermo Scientific) in pyridine (incubated for 60 min at 45 °C) and 15 μl of N-tert-butyldimethylsilyl-N-methyltrifluoroacetamide (MTBSTFA) with 1% tert-butyldimethylchlorosilane (Regis Technologies) and incubated further for 30 min at 45 °C. Derivatives were analyzed by GC—MS using a DB-35MS column (30 m x 0.25 i.d. x 0.25 μm) installed in an Agilent 7890B gas chromatograph (GC) interfaced with an Agilent 5977A mass spectrometer (MS) operating under electron impact ionization at 70 eV. The MS source was maintained at 230 °C and the quadrupole at 150 °C and helium was used as a carrier gas. The GC oven was maintained at 100 °C for 2 min, increased to 300 °C at 10 °C/min and maintained for 4 min, and maintained at 325 °C for 3 min.

2.11. Respirometry

Respiration was measured in adherent monolayers of primary neurons using a Seahorse XFe96 Analyzer with a minimum of 6 biological replicates per plate as previously described [31]. Intact cells were assayed in custom neurobasal medium (ScienCell) supplemented with 5 mM of HEPES, 8 mM of glucose, and 1 mM of pyruvate. Respiration was measured under basal conditions as well as after injection of 2 μM of oligomycin (Oligo), sequential additions of 300 nM of FCCP, and the addition of 0.5 μM of rotenone and 1 μM of antimycin (Ant/Rot). The medium contained 0 mM or 2 mM of itaconate and the pH was adjusted to pH = 7.3 using NaOH. Neurons were incubated in the assay medium for 15 min before starting the assay.

To measure the respiration on specific respiratory substrates, cells were permeabilized with 3 nM of recombinant perfringolysin O (rPFO, commercial XF plasma membrane permeabilizer (PMP), Agilent Technologies) as previously described [35]. Permeabilized neurons were offered oxidizable substrates plus 4 mM of ADP and the initial oxygen consumption was measured, followed by injection of 2 μM of oligomycin (Oligo), sequential additions of 2 μM of FCCP and then the addition of 0.5 μM of rotenone and 1 μM of antimycin (Ant/Rot). Permeabilized neurons were offered 10 mM of succinate with 2 μM of rotenone (Suc/Rot), 5 mM of pyruvate with 1 mM of malate (Pyr/Mal) or 10 mM of ascorbate with 100 μM of TMPD and 1 μM of antimycin A (Asc/TMPD). Maximal respiration was calculated as the difference between protonophore-stimulated respiration (4 μM of FCCP) and non-mitochondrial respiration (measured after the addition of 1 μM of antimycin A and 0.5 μM of rotenone). All of the media were adjusted to pH = 7.3 using KOH.

2.12. RNA isolation and quantitative RT-PCR analysis

Total RNA was purified from cultured cells using a Qiagen RNeasy Mini Kit (Qiagen) per the manufacturer's instructions. First-strand cDNA was synthesized from total RNA using iScript Reverse Transcription Supermix for RT-PCR (Bio-Rad Laboratories) according to the manufacturer's instructions. Individual 10 μl SYBR Green real-time PCR reactions consisted of 1 μl of diluted cDNA, 5 μl of fast SYBR Green Master Mix (Applied Biosystems), and 0.25 μl each of 10 μM forward and reverse primers. To standardize the quantification, b-actin was amplified simultaneously. PCR was carried out in 96-well plates on an Applied Biosystems ViiA 7 Real-Time PCR System using the following parameters: 95 °C for 20 s, 40 cycles of 95 °C for 1 s, and 60 °C for 20 s. *Slc7a11* (forward CCCAGATATGCATCGTCCTT, reverse ACAACCATGAAGAGGCAGGT), *Hmox1* (forward TGACAGAGGAACACAAAGACC, reverse TGAGTGTGAGGACCCATCG), *Gclm* (forward CTGCTAAACTGTTCATTGTAGG, reverse CTATGGGTTTTACCTGTG), *Gsr* (forward CCATGTGGTTACTGCACTTC, reverse CTGAAGCATCTCATCGCAG), *Gpx1* (forward TTGAGAATGTCGCGTCC, reverse AAGCCCAGATACCAGGA), *Nqo1* (forward TGCTTTCAGTTTTCGCCTTT, reverse GAGGCCCCTAATCTGACCTC), *G6pd* (forward GCCTTCTACCCGAAGACACCTT, reverse CTGTTTGCGGATGTCATCCA), beta-actin (forward CGCGAGTACAACCTTCTTGC, reverse CGTCATCCATGGCGAACTGG).

2.13. Immunoblotting

Cells were lysed in ice-cold RIPA buffer supplemented with 1x HALT protease inhibitor cocktail (Thermo Fisher Scientific, Cat. No. 78430). A BCA assay was used to determine the protein concentrations. Overall, 20 μg of total protein was separated on a 4—20% SDS-PAGE gel (mini-protean TGX gels, Bio-Rad) and the proteins were transferred onto a PVDF membrane (Millipore, Cat. No. IPVH10100). The membrane was blocked with 5% non-fat milk in tris-buffered saline with 0.1% Tween 20 (TBS-T) for 1 h and immunoblotted with primary antibody at 4 °C overnight diluted in 5% non-fat milk. Anti-NRF2 (1:1000 dilution, Abcam, Cat. No. ab137550), anti-*Hmox1* (1:1000 dilution, Cell Signaling Technology, Cat. No. E6Z5G), and anti-beta-actin (1:1000 dilution, Cell Signaling Technology, Cat. No. 4970). The immunoblots were then incubated with secondary antibody for 1 h at room temperature (Monoclonal anti-rabbit antibody HRP-conjugate, Cell Signaling Technology, Cat. No 7074, 1:10,000 dilution). Specific signaling was detected using SuperSignal West Pico Chemiluminescent Substrate (Bio-Rad, Cat. No. 1705061) and imaged with a Bio-Rad ChemiDoc XRS + imaging station. Band signaling from Western blotting was determined using ImageJ software and normalized to beta-actin signaling.

2.14. Statistics

Statistical analysis was performed using GraphPad Prism 7. The type and number of replicates and the statistical test used are described in the figure legends. Data are presented as means ± s.e.m. or box (25th to 75th percentile with median line) and whiskers (min. to max. values) as described in the figure legends. A tissue culture was conducted in 12-well tissue culture plates, with each well considered one biological replicate for a given preparation of neurons or astrocytes (minimum of 3 wells per condition). Seahorse assays were performed in 96-well plates, with each well considered a biological replicate (minimum of 6 wells per condition). The mRNA expression was detected with three biological replicates (each with two technical replicates). The protein expression was depicted for three biological replicates. All the data were depicted from one representative experiment and each experiment was repeated one or more times with the exception of the respiratory assay in Figures 1C and 2D as specified in each figure legend.

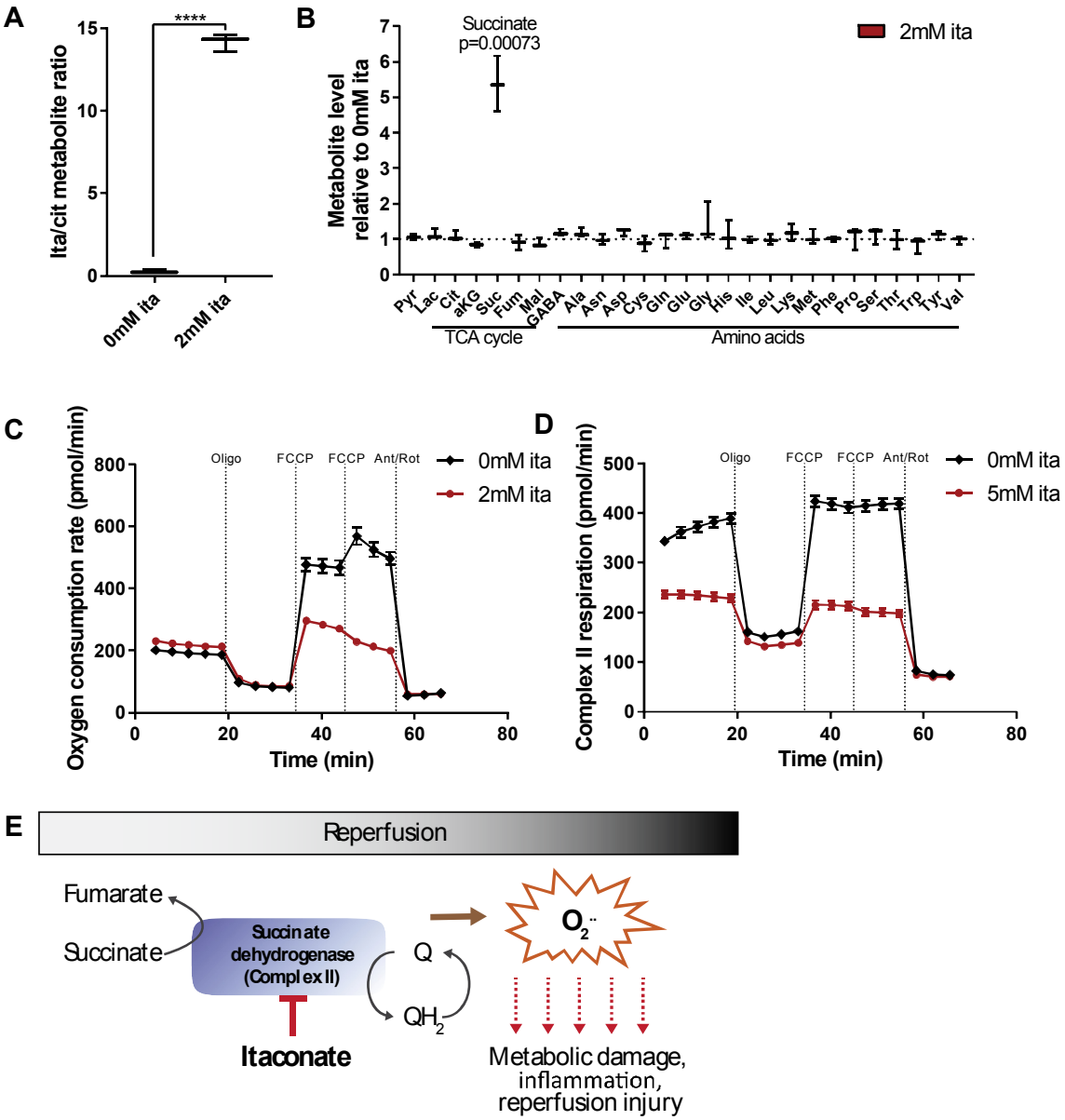

Figure 1: Itaconate inhibited SDH activity in primary cortical neurons. A) Intracellular itaconate levels increased after exposure to 2 mM exogenous itaconate for 2 h. B) Exogenous itaconate drove succinate accumulation while the other metabolites were not affected. Cells were exposed to 2 mM of exogenous itaconate for 2 h. C) Oxygen consumption rate in primary cortical neurons exposed to 2 mM itaconate significantly decreased compared to untreated cells. D) Succinate driven respiration (complex II) in permeabilized primary cortical neurons administered 5 mM succinate and 0.5 μM rotenone. Addition of 5 mM itaconate decreased the oxygen consumption rate. E) Schematic depicting itaconate as a metabolic inhibitor for succinate dehydrogenase (SDH) regulating ROS production upon reperfusion. Data are represented as box (25th to 75th percentile with median line) and whiskers (min. to max. values) with three (A and B) or means ± s.e.m. with 6 biological replicates (C and D). All of the experiments were repeated three independent times with similar results, with the exception of C, which was performed once with 6 biological replicates. Student's *t*-test with $^{****}P < 0.0001$.

In vivo studies were conducted with n = number of male mice aged 9 weeks as indicated in each figure legend. No statistical method was used to predetermine the sample size. *P* values were calculated using Student's two-tailed *t*-test, one-way ANOVA, or two-way ANOVA with a $^{*}P$ value < 0.05, $^{**}P$ value < 0.01, and $^{***}P$ value < 0.001, respectively.

3. RESULTS

3.1. Itaconate inhibits SDH activity in primary cortical neurons

To investigate the biochemical mechanisms by which exogenous itaconate impacts cerebral metabolism, we used primary cultures of rat cortical neurons as a model system. We and others previously demonstrated that extracellular itaconate modulates intracellular metabolism in mammalian cells, including adipocytes, immune cells, and cancer cells [16,17,25,36]. In this study, we supplemented 2 mM of itaconate to cultures of primary cortical neurons for 2 h and quantified the intracellular metabolite levels. Exposure to exogenous itaconate significantly increased the intracellular levels, suggesting that primary cortical neurons took up itaconate from the medium (Figure 1A). Notably, itaconate elevated the intracellular succinate levels by 5-fold, while other metabolites were not affected during this time (Figure 1B). Further, the itaconate and succinate levels increased

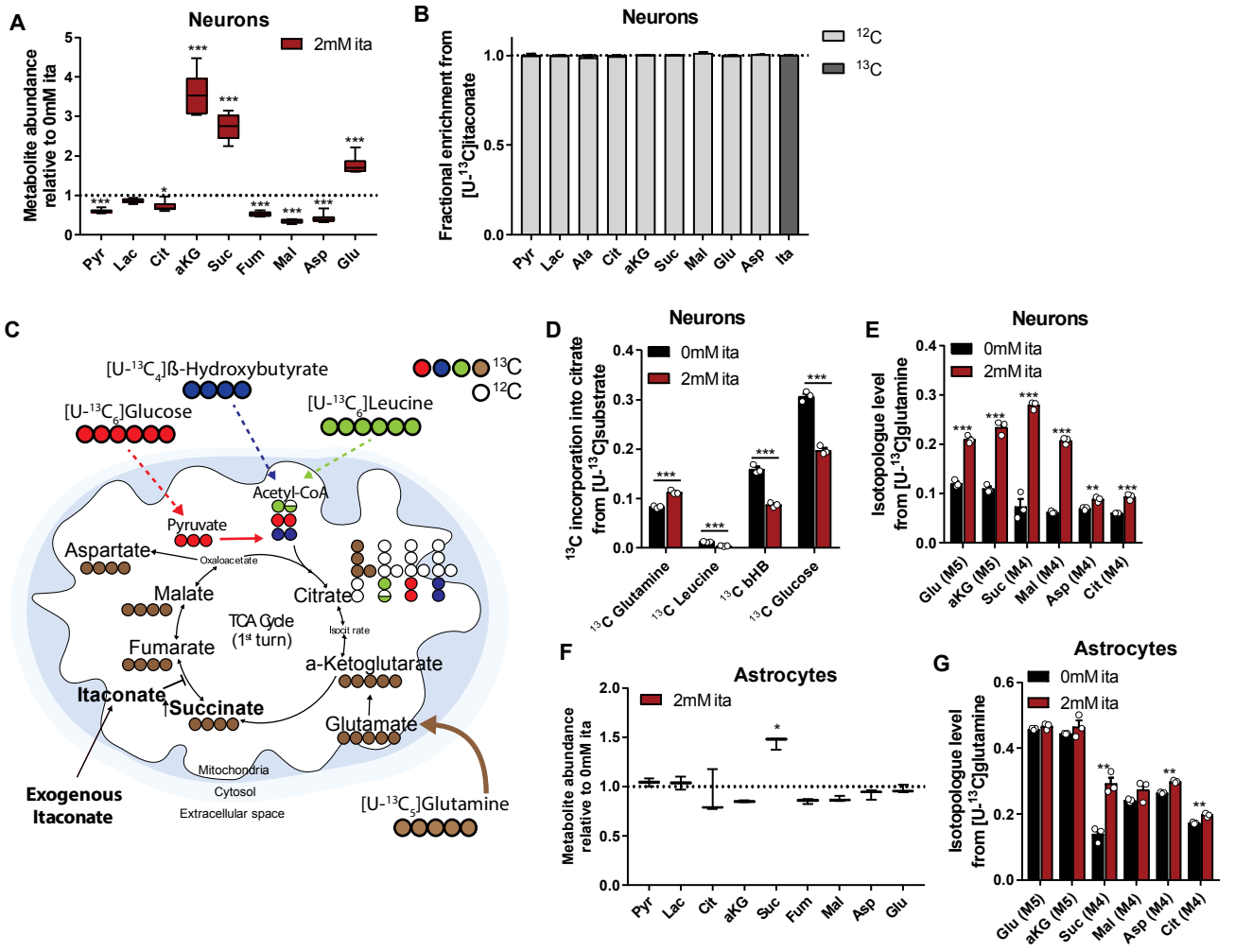

Figure 2: Itaconate impacted substrate utilization for central carbon metabolism and promoted glutamine metabolism in cultured brain cells. A) Relative intracellular metabolite abundances in primary cortical neurons exposed to exogenous itaconate for 48 h. B) Primary cortical neurons did not metabolize ^{13}C itaconate into pyruvate or TCA cycle intermediates in a detectable amount. Cells were exposed to 2 mM [U—^{13}C]itaconate for 48 h and fractional enrichment from ^{13}C itaconate is depicted in dark gray. C) Schematic depicting substrate utilization for TCA cycle metabolism using [U—^{13}C]glucose (red), [U—^{13}C]β-hydroxybutyrate (blue), [U—^{13}C]leucine (green), and [U—^{13}C]glutamine (brown). Open circles depict ^{12}C, and closed circles represent ^{13}C. D) Itaconate decreased ^{13}C incorporation into citrate from ^{13}C substrates [U—^{13}C]leucine (green), [U—^{13}C]β-hydroxybutyrate (blue, bHb), and [U—^{13}C]glucose (red) in primary cortical neurons, while incorporation from [U—^{13}C]glutamine (brown) increased. E) Itaconate increased glutamine metabolism in primary cortical neurons cultured in medium containing [U—^{13}C]glutamine. Graph depicts M4 or M5 labeling on metabolite from ^{13}C glutamine. F) Intracellular metabolite abundances in primary astrocytes exposed to 2 mM exogenous itaconate relative to control condition without itaconate. G) Itaconate increased glutamine metabolism in primary astrocytes cultured in medium containing [U—^{13}C]glutamine. Graph depicts M4 or M5 labeling on metabolite from ^{13}C glutamine. Cells were cultured for 48 h in ^{13}C medium supplemented with 0 mM or 2 mM itaconate. Data are represented as box (25th to 75th percentile with median line) and whiskers (min. to max. values) with six (A) or three (F) biological replicates, or means ± s.e.m. with three biological replicates (B, D, E, and G). All of the experiments were repeated three independent times with the exception of D. Leucine and bHb trace were performed once. Student's *t*-test with $^{*}P < 0.05$, $^{**}P < 0.01$, and $^{***}P < 0.001$.

in a time-dependent manner and correlated positively (Figure S1A-C), suggesting that itaconate drove the observed increase in succinate in the neuronal cultures.

We next assessed whether itaconate impairs the activity of SDH in neurons that may be beneficial for mitigating reperfusion injuries. SDH activity induces reverse electron transport (RET) and ROS production upon reperfusion to promote oxidative stress and cellular injuries [5]. Since SDH (complex II of the electron transport chain) activity helps drive mitochondrial oxygen consumption, we quantified how itaconate impacts neuronal respiration. As depicted in Figure 1C, acute exposure to itaconate decreased uncoupler-stimulated respiration rates in intact primary neurons. In addition, itaconate significantly decreased succinate-driven respiration by complex II (SDH) in permeabilized primary cortical neurons (Figure 1D), while respiration on pyruvate/malate (dependent on complexes I, III, and IV) and ascorbate/TMPD (complex IV) were unaffected (Figure S1D and E). These data indicate that exogenous itaconate specifically inhibits SDH activity and promotes the accumulation of succinate in cultured primary cortical neurons. Thus, itaconate may control the reintroduction of electrons into the mitochondrial electron transport chain upon reperfusion buffering ROS production and metabolic damage (Figure 1E).

3.2. Itaconate promotes glutamine metabolism

The results of this study suggest that itaconate has a direct impact on TCA cycle metabolism. To better understand the long-term impact of itaconate treatment, we exposed cultured neurons to exogenous

itaconate for 48 h. While itaconate significantly increased the intracellular levels of succinate, α-ketoglutarate, and glutamate, there was a significant decrease in the other TCA cycle and glycolytic intermediates, including pyruvate, citrate, and malate (Figure 2A). Notably, we did not detect any ^{13}C labeling on the succinate or other TCA intermediate metabolites in primary neurons exposed to uniformly (U) labeled [U—$^{13}C_5$]itaconate, indicating that cells do not catabolize itaconate appreciably under these conditions (Figure 2B). Further, itaconate in culture medium was not depleted after 48 h (Figure S2A). Our data indicate that itaconate causes an accumulation of metabolites downstream of glutamine, presumably due to SDH inhibition (Figure 1D).

To study itaconate-induced metabolic changes in greater detail, we cultured cortical neurons in the presence of ^{13}C isotope tracers and quantified the isotope enrichment throughout the metabolome. We cultured primary cortical neurons in custom Neurobasal-C medium lacking specific substrates to enable replacement with isotopic labeled tracers such as [U—$^{13}C_6$]glucose, [U—$^{13}C_5$]glutamine, [U—$^{13}C_4$]β-hydroxybutyrate, and [U—$^{13}C_6$]leucine. Each of these substrates was significantly oxidized by the primary cortical neurons [31]. For glutamine tracer studies, we included the N-methyl-D-aspartate (NMDA) receptor antagonist MK801 to prevent excitotoxic neuronal injury from glutamine deamination [31]. While carbons derived from β-hydroxybutyrate, leucine, and glucose enter the TCA cycle primarily via acetyl-CoA, glutamine is converted into glutamate that is further metabolized to α-ketoglutarate (Figure 2C). To compare substrate utilization across different carbon sources, we cultured primary neurons in ^{13}C tracer medium supplemented with 0 mM or 2 mM of itaconate for 48 h and quantified labeling on citrate. Exogenous itaconate significantly decreased neuronal glucose oxidation while increasing oxidative glutamine metabolism (Figure 2D). We also observed decreased ^{13}C incorporation into the citrate from ^{13}C labeled leucine and β-hydroxybutyrate, evidence that itaconate influences mitochondrial substrate utilization (Figure 2D).

Acute (2 h) exposure to itaconate significantly increased labeling on succinate from [U—$^{13}C_5$]glutamine while ^{13}C incorporation into the other TCA cycle intermediates was not affected (Figure S2B and C). However, long-term exposure to itaconate significantly increased isotope enrichment on the other TCA cycle intermediates and related amino acids from [U—$^{13}C_5$]glutamine (Figure 2E and Figure S2D-H) while decreasing glucose oxidation (Figure S2I), presumably due to the slow progressing oxidation of glutamine-derived succinate that occurred during this prolonged time period.

Because the brain comprised of diverse cells with distinct metabolic phenotypes, we also quantified the impact of exogenous itaconate on primary rat cortical astrocytes. Similar to neuronal cultures, itaconate was not catabolized into the TCA cycle intermediates (Figure S2J) but did promote succinate accumulation (Figure 2F) and glutamine flux to succinate (Figure 2G and S2K) in cultured astrocytes after 48 h of culture. While itaconate treatment increased the succinate levels in the astrocytes, the other TCA cycle intermediates were not affected, suggesting that distinct metabolic reprograming occurred in the astrocytes and neurons. Collectively, our data indicate that itaconate reprograms intermediary metabolism, specifically glutamine metabolism, in primary cortical neurons and astrocytes, which may be beneficial for improving metabolic homeostasis in ischemia reperfusion.

3.3. Activation of anti-oxidant cell response via itaconate in primary brain cells

Based on this study's metabolic data, we hypothesized that itaconate promotes glutamine metabolism for anti-oxidant defense pathways. Synthetic, cell-permeable derivatives of itaconate (that is, octyl-itaconate and dimethyl-itaconate) can buffer inflammation and redox homeostasis in immune cells via Nrf2 and ATF3 [24,25]. Nrf2 is a transcription factor and key regulator of redox homeostasis that protects from oxidative stresses by stimulating the expression of genes involved in heme metabolism (heme-oxygenase-1 (*Hmox1*)) and ROS detoxification (NAD(P)H dehydrogenase (*Nqo1*)). In addition, Nrf2 contributes to cellular metabolic activities and drives the transcription of metabolic genes advantageous for proliferation and survival [37]. In fact, Nrf2 target genes encode numerous enzymes involved in glutamine and glutathione metabolism, including glutathione peroxidase 1 (*Gpx1*) [38—41].

Since anti-oxidant responses are critical for mitigating reperfusion injury [27,42], we next determined whether itaconate activates the anti-oxidant related gene signaling pathway in primary cortical neurons or astrocytes. To assess this, we quantified the expression of redox-associated genes in our cell model of primary cultured brain cells in response to itaconate treatment. In neuronal cultures, exogenous itaconate significantly increased the expression levels of genes associated with redox metabolism, specifically *Hmox1* (3.3-fold increase), *Nqo1* (4.5-fold increase), and *Gpx1* (2-fold increase) (Figure 3A). Further, itaconate increased the protein levels of NRF2 by 1.5-fold and HMOX1 by 1.6-fold (Figure 3B,C). However, the expression of these genes was not dramatically affected in the primary astrocytes (Figure 3D). Furthermore, some classical Nrf2 targets such as glucose-6-phosphate dehydrogenase (*G6pd*) were not upregulated in the neurons (Figure 3A,D), suggesting that the transcriptional response of neurons/astrocytes to itaconate is distinct from that occurring in immune cells [24,25]. Collectively, we observed changes in the redox-associated pathways in the cultured neurons, suggesting that itaconate strongly influences glutamine metabolism that is critical for anti-oxidant defense mechanisms (Figure 3E).

3.4. Itaconate modulates brain redox metabolism in a cerebral ischemia-reperfusion model

Given its influence on SDH activity, glutamine metabolism, and anti-oxidant pathway induction, we hypothesized that the administration of itaconate prior to reperfusion might have protective effects in animal models of cerebral ischemia. To explore this, we infused mice with itaconate (15 mg/kg/min) for 30 min prior to inducing ischemia via middle cerebral artery (MCA) and common carotid artery (CCA) neural ligation and again for 30 min during reperfusion (Figure 4A). The vehicle group was infused with 0.9% NaCl and the sham group underwent surgery but without ligation. Plasma itaconate reached 2 mM 2 h after reperfusion but was not detectable in the control condition or treated animal plasma 24 h after reperfusion, indicating that this compound cleared rapidly in the mice (Figure 4B). We also observed that pyruvate, lactate, TCA cycle intermediates, and amino acids were elevated in the vehicle control groups 24 h after reperfusion compared to baseline, suggesting that they could serve as biomarkers of reperfusion injury [43]. Intriguingly, these metabolites were not altered in the plasma from the itaconate-infused mice at the same time point (Figure 4C and Figure S3A and B). These data suggest that exogenous itaconate impacts intermediary metabolism in vivo and buffers against metabolic alterations associated with reperfusion.

We next investigated the impact of itaconate on oxidative stress markers after reperfusion injury. The total glutathione levels in the brain were significantly decreased in the vehicle group compared to the sham conditions but were not altered in the itaconate-treated animals (Figure 4D). Reduced glutathione (GSH) is a vital protective anti-oxidant, and the itaconate significantly elevated the GSH levels compared to the vehicle group (Figure 4E). Further, the oxidized

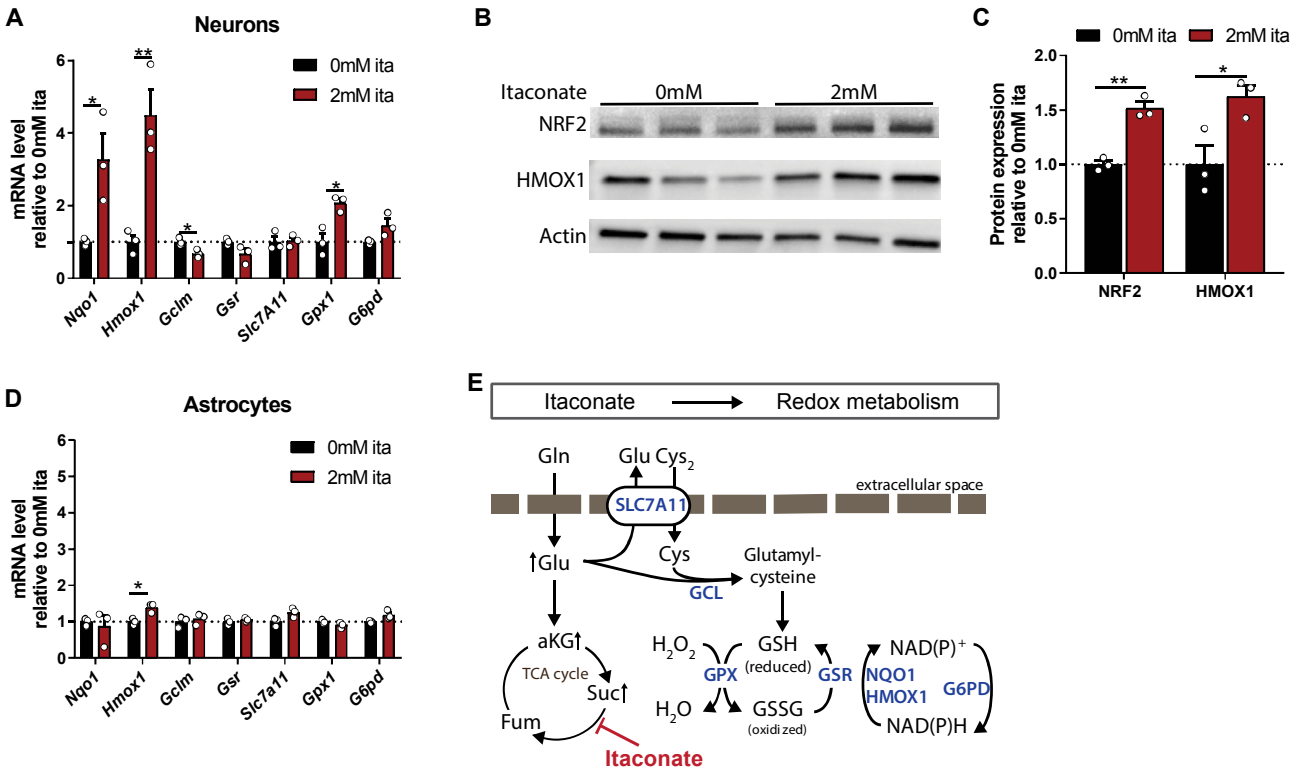

Figure 3: Itaconate induced anti-oxidant cell response in primary brain cells. A) Itaconate induced expression of anti-oxidant-related genes in primary cortical neurons. B) NRF2, HMOX1, and actin protein expression in primary cortical neurons depicted as Western blotting. C) NRF2 and HMOX1 protein expression in primary cortical neurons depicted as band intensity normalized to actin (from Western blotting depicted in B). D) Expression of anti-oxidant related genes in primary astrocytes. E) Schematic overview of proteins involved in oxidative stress response. *Slc7a11*: cystine-glutamate transporter; *Gclm*: glutamate-cysteine ligase; *Gsr*: glutathione reductase; *Gpx1*: glutathione peroxidase 1; *Nqo1*: NAD(P)H dehydrogenase; *G6pd*: glucose-6-phosphate dehydrogenase; *Hmox1*: heme oxygenase 1. Cells were exposed to 2 mM exogenous itaconate for 48 h. Data are represented as means ± s.e.m. with three biological replicates (with two technical replicates for each gene expression study). All of the experiments were repeated two independent times with similar results. Student's *t*-test with $*P < 0.05$ and $**P < 0.01$.

glutathione levels (GSSG) were significantly increased in the vehicle group but not in the itaconate group while the GSH/GSSG ratios were significantly decreased upon itaconate treatment compared to the sham conditions (Figure 4F,G). Our data indicate that itaconate protects against glutathione depletion and improves the anti-oxidant capacity of cells (Figure 4F,G). Furthermore, itaconate decreased the NADH/NAD^+ ratio in the brain 2 h after reperfusion (Figure 4H), providing evidence that oxidative metabolism is better maintained when itaconate is administered prior to neural ligation and during reperfusion. Importantly, itaconate also reduced the cerebral ROS/RNS levels compared to the vehicle-treated controls as measured by oxidant-sensitive dihydrorhodamine-123 (DHR-123) fluorescent probes (Figure 4I). These data suggest that itaconate elicits beneficial metabolic effects when applied to in vivo models of reperfusion injury.

3.5. Itaconate improves hemodynamics and brain function after reperfusion injury

Reperfusion injury can also compromise cerebral blood flow, contributing to further tissue damage due to impaired oxygen and nutrient delivery. To directly investigate the impact of itaconate on cerebral hemodynamics and microvascular function, we used a closed cranial window chamber that allowed us to monitor vascular function within the brain after reperfusion in real time. Specifically, we measured the critical microvascular parameters involved in ischemia-reperfusion injury, that is, arteriolar diameter, blood flow, and leukocyte adhesion. Itaconate prevented arteriolar vessel collapse (Figure 5A and S4A), improved arterial blood flow (Figure 5B and S4B), and preserved cerebral oxygen tension (Figure 5C) 2 h after reperfusion compared to the vehicle-treated and sham control groups. Our data indicate that itaconate prevents cerebral vasoconstriction during reperfusion, which preserves cerebral blood flow and oxygen supply critical for tissue oxygenation and function. Cerebral vasospasm is an important cause of morbidity during ischemia reperfusion that is independently associated with reduced instrumental activities of daily living, cognitive impairment, and poor quality of life [44]. Importantly, itaconate's effects on blood flow-mediated oxygenation and nutrient supply were as effective as emergent endovascular spasmolysis and vasodilators [45].

We next sought to determine whether itaconate reduces inflammation associated with reperfusion in vivo. Reperfusion induces an inflammatory response impacting brain edema formation. Comparison of the sham and vehicle groups demonstrated that ischemia-reperfusion injury increased brain edema by 4.7%. Itaconate administration significantly mitigated this increase to 1.8% such that the itaconate cohort was not different than the sham group (Figure 5D). Reperfusion increases leukocyte-endothelial adhesion, a hallmark of neural inflammation. Therefore, we quantified leukocyte adhesion to the vascular endothelium at baseline and 2 h post-reperfusion using our mouse cranial window chamber model. Supplementation of itaconate in reperfusion fluid significantly decreased the number of rolling

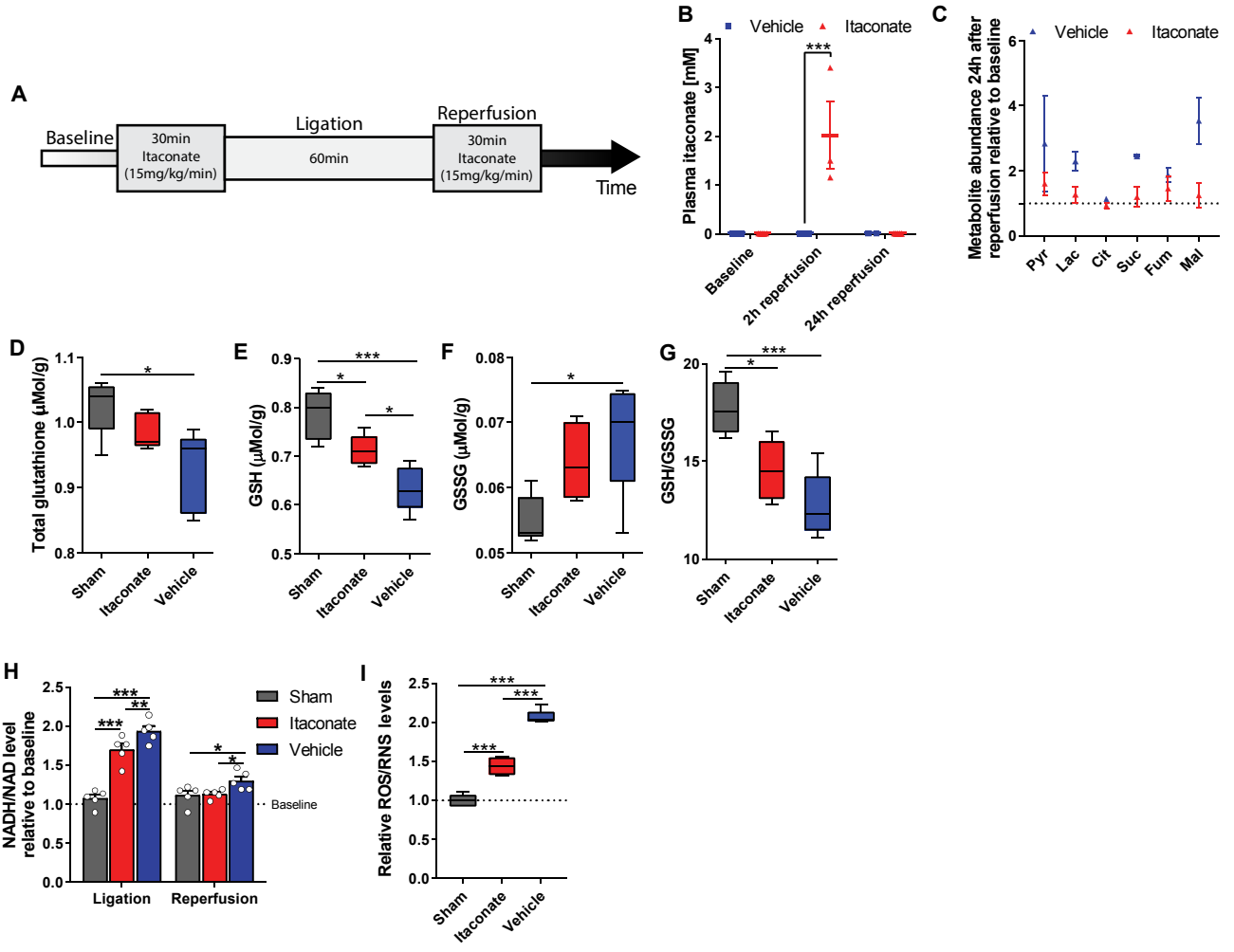

Figure 4: Itaconate modulated brain redox metabolism in a cerebral ischemia-reperfusion model. A) Experimental overview of a mouse animal model of acute cerebral ischemia. Mice were infused with NaCl (vehicle, blue), or itaconate (15 mg/kg/min, red) for 30 min prior to ligation. 60 min after ligation, reperfusion was initiated and the mice were infused again for 30 min. B) Plasma itaconate levels 2 and 24 h after reperfusion. C) Plasma metabolite levels 24 h after reperfusion in vehicle compared to itaconate-treated group relative to baseline. D) Total glutathione levels in brain tissue 24 h after reperfusion. E) Reduced glutathione (GSH) levels in brain tissue 24 h after reperfusion. F) Oxidized glutathione (GSSG) levels in brain tissue 24 h after reperfusion. G) GSH (reduced)/GSSG (oxidized) glutathione levels in brain tissue 24 h after reperfusion. H) Reduction potential (NADH/NAD ratio) indicating mitochondrial oxidative phosphorylation 2 h after reperfusion relative to baseline. I) Reactive oxygen/nitrogen species (ROS/RNS) in brain tissue 2 h after reperfusion. Data are represented as box (25th to 75th percentile with median line) and whiskers (min. to max. values) (B, D-G, and I) or means ± s.e.m. (C and H). Experiments were performed with n = number of male mice aged 9 weeks. Two-way ANOVA (B with n = 2 for vehicle and n = 5 for itaconate; H, n = 5) or one-way ANOVA (D-G and I, n = 5) with $^{*}P < 0.05$, $^{**}P < 0.01$, and $^{***}P < 0.001$.

leukocytes after 2 h, providing additional evidence that itaconate reduced inflammation relative to the vehicle-treated control conditions (Figure 5E). Importantly, leukocyte-endothelial adhesion is regulated by inflammatory adhesion molecules, which are regulated by oxidative stress. Oxidative stress can regulate the expression of endothelial cell adhesion molecules (CAMs) by a direct activation of CAMs and transcription factors (that is, NF-κB and AP-1). In addition to oxidative stress, inflammatory mediators such as thrombin, VEGF, IL-17, and TNF-α are known to enhance the surface expression of CAM P-selectin to mediate leukocyte adhesion [46]. Therefore, our data suggest an important role for itaconate in decreasing redox stress, inflammation, and leukocyte-endothelial interaction associated with ischemia-reperfusion injuries.

Given the positive effects of itaconate on metabolism, hemodynamics, and inflammation, we next tested whether itaconate affects overall brain function and quantified neurological behavior following ischemia and reperfusion. While reperfusion significantly decreased motor and behavioral function in the vehicle compared to the sham groups, the itaconate-treated group was not significantly different from the sham animals (Figure 5F). Collectively, these results provide evidence that itaconate protects the brain against reperfusion injury by influencing redox metabolism, blood flow, and oxygen delivery, reducing inflammation and improving overall brain function in a mouse model of neural ischemia-reperfusion injury. These promising pre-clinical data warrant further investigation in additional animal models and species along with an evaluation of the therapeutic window.

3.6. Itaconate reduces mortality from TBI with hemorrhagic shock

To assess whether itaconate mitigates more severe cerebral reperfusion injuries, we examined the physiological benefits of itaconate when supplemented to resuscitation fluids used to treat TBI followed by hemorrhagic shock resuscitation. The immediate goal of current

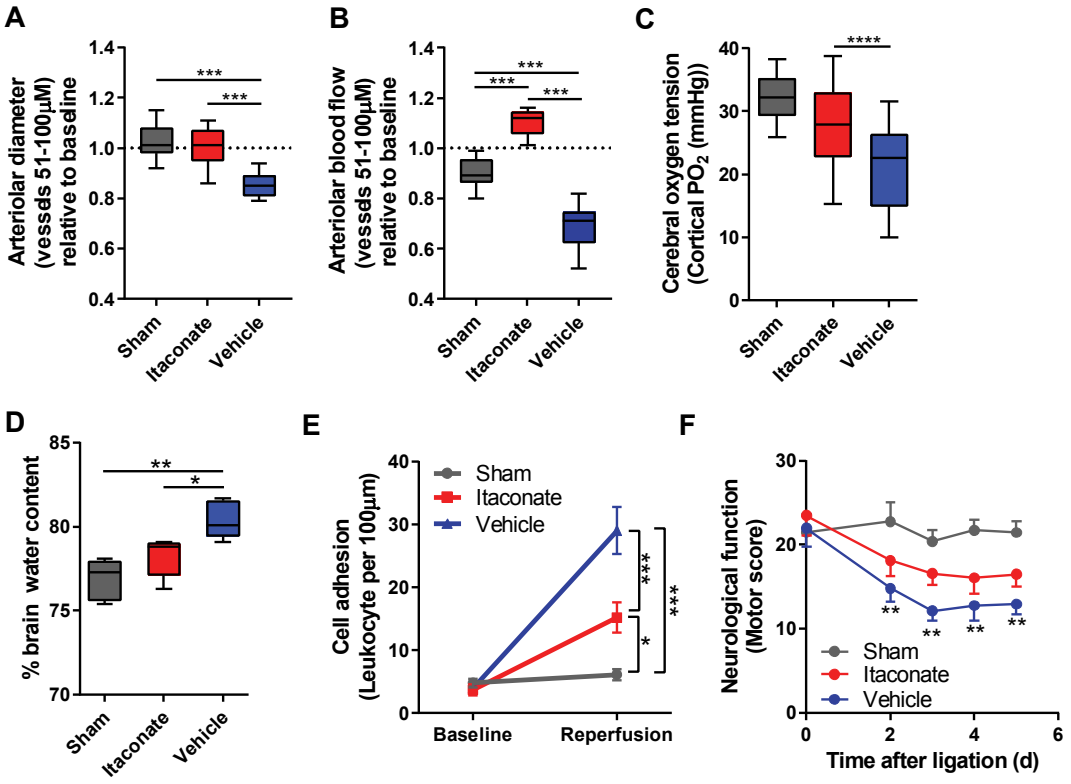

Figure 5: Itaconate improved hemodynamics and brain function after reperfusion injury. A) Cerebral arteriolar diameter 2 h after reperfusion in cranial window model. B) Cerebral arteriolar blood flow 2 h after reperfusion in cranial window model. C) Itaconate increased cerebral oxygen tension 2 h after reperfusion. D) Brain edema 24 h after reperfusion is shown as % water content in brain considering brain weights (mg) (mean ± s.e.m.) of the sham (458.6 mg ± 5.6 mg), itaconate (475.0 mg ± 6.3 mg), and vehicle (503.6 ± 8.1 mg) groups. E) Leukocyte adhesion as a parameter for inflammation significantly decreased in itaconate-infused group 2 h after reperfusion compared to control groups. F) Infusion of itaconate improved neurological scores upon reperfusion. Data are represented as box (25th to 75th percentile with median line) and whiskers (min. to max. values) (A, B, C, and D) or means ± s.e.m. (E and F). Experiments were performed with n = number of male mice aged 9 weeks. A, B, n = 6 mice with 14–16 analyzed blood vessels; C, D, F: n = 5; E, n = 4). One-way ANOVA (A–D) or two-way ANOVA (E and F), with $^{*}P < 0.05$, $^{**}P < 0.01$, and $^{***}P < 0.001$.

treatments for TBI with trauma is to provide fluid resuscitation to maintain consciousness and central nervous system activity. We used a mouse model of fluid percussion TBI followed by 50% of the animal's blood volume hemorrhage that resulted in a decrease in the mean arterial pressure (MAP) to 35–40 mmHg (Figure 6A). We then provided volume fluid resuscitation to maintain MAP above 70 mmHg using lactated Ringer's solution (LR), blood plasma volume expander Hextend, or Hextend supplemented with 15 mg/mL of water-soluble itaconate. The MAP was not affected by the choice of resuscitation fluid (Figure 6A). Notably, inclusion of itaconate slightly reduced the total resuscitation volume required to preserve the MAP compared to the control group with Hextend alone, suggesting that itaconate may

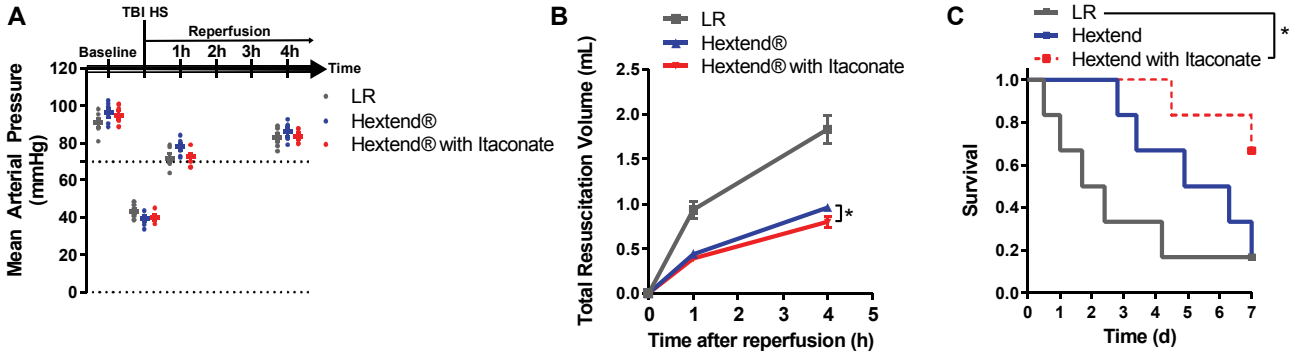

Figure 6: Itaconate reduced mortality from TBI with hemorrhagic shock. A) Mice were subjected to fluid percussion TBI followed by hemorrhage of 50% of the animal's blood volume. Volume resuscitation was accomplished by preserving the mean arterial pressure (MAP) above 70 mmHg for 4 h. Fluid resuscitation was accomplished using lactated Ringer's solution (LR), plasma expander Hextend, or Hextend supplemented with 15 mg/ml itaconate. B) Total resuscitation volume used to maintain the MAP above 70 mmHg 1 and 4 h after reperfusion in control groups compared to itaconate-infused group. Data are represented as means ± s.e.m., with Student's *t*-test $^{*}P < 0.05$ 4 h after reperfusion. C) Itaconate improved survival rates in a mouse model of TBI/shock (67% survival) compared to control groups with lactated Ringer's solution (LR) and plasma expander Hextend (17% survival). $^{*}P < 0.05$. Experiments were performed with all groups n = 6 male mice aged 9 weeks.

decrease the dilution of clotting factors in the blood, reducing the risk of additional hemorrhage (Figure 6B). Finally, itaconate significantly increased survival rates 7 days after reperfusion compared to the control group (66.7% vs 16.7% survival), indicating that itaconate impacts physiology to improve overall outcomes in reperfusion injuries (Figure 6C). These data correlate with evidence of increased tissue oxygenation, reperfusion, and metabolic recovery in animal models of trauma and metabolic reprogramming in cultured neurons, supporting the concept that itaconate improves physiological outcomes associated with reperfusion injury.

4. DISCUSSION

In this study, we demonstrated that inclusion of itaconate in resuscitation fluids limits reperfusion-induced injurious metabolic processes. Our findings integrate distinct physiological benefits in animal models with molecular analysis in cultured brain cells, highlighting the regulation of metabolic pathways and anti-oxidant response by itaconate. Cerebral ischemic conditions limit nutrient and oxygen supply for brain metabolism, impacting numerous biochemical pathways. Reperfusion of ischemic tissue drives the production of mitochondrial superoxide [47–51]. For example, high levels of succinate have been detected in multiple tissues under ischemic conditions, and after reperfusion, this accumulated succinate is rapidly oxidized by SDH, resulting in increased mitochondrial ROS production and damage [4,5,52]. In this study, we demonstrated that itaconate decreases SDH activity in brain cells (Figure 1D) and reduces ROS/RNS levels upon reperfusion in vivo (Figure 4I), suggesting that targeting this enzyme complex may buffer against the oxidative damage that occurs under such conditions. The first few minutes of reperfusion are critical as they initiate long-term tissue damage and dysfunction [1]. Inhibitors of SDH, that is, dimethyl malonate and atpenin A5, have been shown to ameliorate reperfusion injuries in a variety of in vivo models [5,53,54]. Importantly, in our current study, the respiratory chain remained partially inhibited upon itaconate infusion during reperfusion, and itaconate-dependent regulation of SDH activity resulted in a gradual "awakening" of mitochondrial metabolism after reperfusion. Thus, itaconate may inhibit mitochondrial superoxide formation by slowing (but not halting) the reintroduction of electrons into the mitochondrial electron transport chain upon reperfusion [51]. Importantly, our data indicate that itaconate is cleared from the plasma within 24 h after reperfusion (Figure 4B), which should permit full recovery of SDH activity and respiratory function that is important for recovery after such injuries.

To neutralize free oxygen radicals during reperfusion, cells activate anti-oxidant responses. Nrf2 is a transcription factor of the endogenous anti-oxidant response and is recognized as a regulator of cellular metabolism to fulfill the increased cellular glutamate demand for glutathione synthesis [38–40,55,56]. In our study, itaconate promoted redox metabolism and reprogrammed glutamine metabolism in vitro and in vivo. Since itaconate increased glutamine use in the TCA cycle in the cultured neurons, this molecule could promote the oxidation of alternate substrates during reperfusion when glucose availability is limited. Itaconate significantly reduced inflammation-induced brain damage and increased neurological function, which may be attributed to the regulation of neuronal anti-oxidant response and SDH inhibition induced by exogenous itaconate. In addition, carboxylic acids, such as pyruvate, are effective ROS scavengers [57] and therefore itaconate itself may function as an endogenous anti-oxidant molecule limiting the cytopathic effects of reduced forms of oxygen. Thus, itaconate-dependent metabolic regulation could mitigate reperfusion injuries or benefit other diseases driven by oxidative stress.

We observed that plasma itaconate cleared within 24 h, suggesting that it is readily metabolized in vivo (Figure 4B). Thus, itaconate and/or its degradation products may also affect the metabolic function of diverse cell types and tissues. The liver is likely the primary site of itaconate degradation, which occurs via activation to itaconyl-CoA and further breakdown into pyruvate and acetyl-CoA, and this metabolic process has been observed in isolated liver mitochondria [58]. However, our tracer study indicated that the cultured brain cells did not catabolize itaconate into TCA cycle intermediates in detectable amounts, similar to macrophages and cancer cells [16]. Alternatively, itaconate might be secreted in urine as observed in dogs and rats [59,60]. Itaconate and its potential metabolic products are likely to alter cellular function in multiple organs at a system level to limit the pathological consequences of diseases. For instance, since itaconate reduced ROS/RNS levels (Figure 4I) and prevented collapse of blood vessels in our in vivo animal model (Figure 5B), itaconate might also reprogram endothelial metabolism and affect nitric oxide synthase (NOS) expression and/or nitric oxide (NO) production to promote further protection in ischemia reperfusion.

The immediate goals of treating brain injuries are optimizing cerebral blood flow and oxygenation, minimizing intracranial pressure fluctuations, and reducing cerebral edema [6]. However, intravenous infusion of fluids (colloids and crystalloids) dilutes clotting factors causing additional injury [61]. Our data indicate that itaconate reduces the extent of tissue damage caused by ischemia and TBI/hemorrhagic shock, the resulting oxygen insufficiency, and the adverse consequences of reperfusion injury; all of which are characterized by the development of both localized and systemic oxidative stress driving cell death. Further, our results suggest that itaconate may add cellular protection to the fluid resuscitation strategy to maintain body function, thereby improving outcomes. Thus, itaconate is a central factor to mitigate reperfusion-induced injuries and a target for intervention.

Our results indicate considerable promise for the translation of an itaconate-based treatment strategy to mitigate reperfusion injuries, yet there are several limitations to our study. All of the intervention studies were conducted in male mouse models, and the potential translational relevance of itaconate in humans requires formal testing in a time- and dose-dependent manner. Human CAD/IRG1 is less active than the murine enzyme, in part due to naturally occurring mutations [21]. Deficiency of CLYBL enzyme impairs itaconate degradation and impacts B_{12} metabolism [36]. These changes could influence the ability of patients to safely process itaconate. Thus, factors such as sex and genetic background must also be considered in future studies. Indeed, the impact of exogenous itaconate may differ by sex as macrophages from estrogen-deficient mice synthesize less endogenous itaconate than wild-type mice [62]. Notably, itaconate was administered prior to initiating ischemic injury (and reperfusion) in our mouse model of IR rather than after the primary injury occurred. However, we administered itaconate after the primary injury and during reperfusion in our model of TBI/HS supporting the hypothesis that the Nrf2 preconditioning effect might not be the key phenotypic driver. Rather, our results support the concept that rapid SDH inhibition might be most effective for protection. Future studies will explore itaconate administration scheduling and propose strategies in more detail. However, itaconate is a natural molecule that has a long shelf life and is soluble. SDH activity has emerged as a focal point of investigation for diverse metabolic diseases beyond reperfusion injuries, including cancer [63,64], neurodegeneration [65], and inflammation [16,17,66]. Since itaconate impairs SDH activity in a number of different cell types [16,17,67], itaconate may accelerate important progress in clinical medicine. However, since itaconate has only recently been described

as an endogenous metabolite, we are still beginning to understand its functional impacts in different cell types.

5. CONCLUSIONS

Collectively, our study supports continued research in this area and demonstrates that exogenous itaconate favorably modifies the host response to ischemia and reperfusion that is sufficient to suppress reperfusion-related injuries. These are the first studies of exogenous itaconate treatment that could be an important new strategy to increase intracellular itaconate levels in vital organs to improve metabolic homeostasis in ischemia and reperfusion. We believe that our results might add significantly to the current understanding of the clinical experience with identification and verification of therapeutic efficacy of a new itaconate-based treatment strategy to reduce cellular injuries in the response to ischemia and reoxygenation.

AUTHOR CONTRIBUTION

T.C., C.M.M., and P.C. devised and coordinated the project. T.C. designed, analyzed, and conducted the experiments with cultured brain cells with the assistance of A.N.M. T.C. and P.C. performed and analyzed the in vivo animal studies. A.L. and A.S.D. provided expert technical assistance. T.C. and C.M.M. wrote the manuscript with the assistance of all of the authors.

DATA AND MATERIAL AVAILABILITY

All of the data associated with this study are in the paper or Supplementary Materials.

ACKNOWLEDGMENTS

We thank all of the members of the Metallo and Cabrales Laboratories, United States for support and helpful discussions. We thank the NIH Common Fund Metabolite Standards Synthesis Core (NHLBI contract no. HHSN268201300022C) for providing isotopic labeled itaconate ([U−$^{13}C_5$]itaconate). This study was supported, in part, by US National Institutes of Health (NIH) grants R01CA188652 and R01CA234245 (C.M.M.), NSF CAREER Award #1454425 (C.M.M.), a Camille and Henry Dreyfus Teacher-Scholar Award (C.M.M.), NIH grants R01 HL126945 NHLBI (P.C.), R01 HL138116 NHLBI (P.C.), R01NS087611 NINDS (A.N.M.), R21NS104513 NINDS (A.N.M.), and Deutsche Forschungsgesellschaft, Germany (German Research Foundation) (CO1488/1-1 to T.C).

CONFLICT OF INTEREST

The authors declare that they have no conflicts of interest with the content of this article.

APPENDIX A. SUPPLEMENTARY DATA

Supplementary data to this article can be found online at https://doi.org/10.1016/j.molmet.2019.11.019.

REFERENCES

[1] Eltzschig, H.K., Eckle, T., 2011. Ischemia and reperfusion-from mechanism to translation. Nature Medicine 17(11):1391–1401. https://doi.org/10.1038/nm.2507.

[2] White, B.C., Sullivan, J.M., DeGracia, D.J., O'Neil, B.J., Neumar, R.W., Grossman, L.I., et al., 2000. Brain ischemia and reperfusion: molecular mechanisms of neuronal injury. Journal of the Neurological Sciences 179(S 1–2):1–33. https://doi.org/10.1016/S0022-510X(00)00386-5.

[3] McCord, J.M., 1987. Oxygen-derived radicals: a link between reperfusion injury and inflammation. Federation Proceedings.

[4] Chouchani, E.T., Pell, V.R., James, A.M., Work, L.M., Saeb-Parsy, K., Frezza, C., et al., 2016. A unifying mechanism for mitochondrial superoxide production during ischemia-reperfusion injury. Cell Metabolism 23(2):254–263. https://doi.org/10.1016/j.cmet.2015.12.009.

[5] Chouchani, E.T., Pell, V.R., Gaude, E., Aksentijević, D., Sundier, S.Y., Robb, E.L., et al., 2014. Ischaemic accumulation of succinate controls reperfusion injury through mitochondrial ROS. Nature 515(7527):431–435. https://doi.org/10.1038/nature13909.

[6] Toledo-Pereyra, L.H., Toledo, A.H., Walsh, J., Lopez-Neblina, F., 2004. Molecular signaling pathways in ischemia/reperfusion. Experimental and Clinical Transplantation :Official Journal of the Middle East Society for Organ Transplantation 2(1):174–177.

[7] Andreyev, A., Tamrakar, P., Rosenthal, R.E., Fiskum, G., 2018. Calcium uptake and cytochrome c release from normal and ischemic brain mitochondria. Neurochemistry International 117:15–22. https://doi.org/10.1016/j.neuint.2017.10.003.

[8] Balan, I.S., Saladino, A.J., Aarabi, B., Castellani, R.J., Wade, C., Stein, D.M., et al., 2013. Cellular alterations in human traumatic brain injury: changes in mitochondrial morphology reflect regional levels of injury severity. Journal of Neurotrauma 30(5):367–381. https://doi.org/10.1089/neu.2012.2339.

[9] Martínez-Reyes, I., Diebold, L.P., Kong, H., Schieber, M., Huang, H., Hensley, C.T., et al., 2016. TCA cycle and mitochondrial membrane potential are necessary for diverse biological functions. Molecular Cell 61(2):199–209. https://doi.org/10.1016/J.MOLCEL.2015.12.002.

[10] Carden, D.L., Granger, D.N., 2000. Pathophysiology of ischaemia-reperfusion injury. The Journal of Pathology 190(3):255–266. https://doi.org/10.1002/(SICI)1096-9896(200002)190:3<255::AID-PATH526>3.0.CO;2-6.

[11] Rothman, S.M., Olney, J.W., 1986. Glutamate and the pathophysiology of hypoxic-ischemic brain damage. Annals of Neurology 19(2):105–111. https://doi.org/10.1002/ana.410190202.

[12] Prakash, A., Sundar, S.V., Zhu, Y.-G., Tran, A., Lee, J.-W., Lowell, C., et al., 2015. Lung ischemia-reperfusion is a sterile inflammatory process influenced by commensal microbiota in mice. Shock (Augusta, Ga.) 44(3):272–279. https://doi.org/10.1097/SHK.0000000000000415.

[13] Dekker, S.E., Nikolian, V.C., Sillesen, M., Bambakidis, T., Schober, P., Alam, H.B., 2018. Different resuscitation strategies and novel pharmacologic treatment with valproic acid in traumatic brain injury. Journal of Neuroscience Research 96(4):711–719. https://doi.org/10.1002/jnr.24125.

[14] Wilhelmsen, K., Khakpour, S., Tran, A., Sheehan, K., Schumacher, M., Xu, F., et al., 2014. The endocannabinoid/endovanilloid N-arachidonoyl dopamine (NADA) and synthetic cannabinoid WIN55,212-2 abate the inflammatory activation of human endothelial cells. Journal of Biological Chemistry 289(19):13079–13100. https://doi.org/10.1074/jbc.M113.536953.

[15] Hall, E.D., Vaishnav, R.A., Mustafa, A.G., 2010. Antioxidant therapies for traumatic brain injury. Neurotherapeutics 7(1):51–61. https://doi.org/10.1016/j.nurt.2009.10.021.

[16] Cordes, T., Wallace, M., Michelucci, A., Divakaruni, A.S., Sapcariu, S.C., Sousa, C., et al., 2016. Immunoresponsive gene 1 and itaconate inhibit succinate dehydrogenase to modulate intracellular succinate levels. Journal of Biological Chemistry 291(27):14274–14284. https://doi.org/10.1074/jbc.M115.685792.

[17] Lampropoulou, V., Sergushichev, A., Bambouskova, M., Nair, S., Vincent, E.E., Loginicheva, E., et al., 2016. Itaconate links inhibition of succinate dehydrogenase with macrophage metabolic remodeling and regulation of inflammation. Cell Metabolism 24(1):1–9. https://doi.org/10.1016/j.cmet.2016.06.004.

[18] Michelucci, A., Cordes, T., Ghelfi, J., Pailot, A., Reiling, N., Goldmann, O., et al., 2013. Immune-responsive gene 1 protein links metabolism to immunity by catalyzing itaconic acid production. Proceedings of the National Academy of Sciences of the United States of America 110(19):7820–7825. https://doi.org/10.1073/pnas.1218599110.

[19] Strelko, C.L., Lu, W., Dufort, F.J., Seyfried, T.N., Chiles, T.C., Rabinowitz, J.D., et al., 2011. Itaconic acid is a mammalian metabolite induced during macrophage activation. Journal of the American Chemical Society 133(41): 16386–16389. https://doi.org/10.1021/ja2070889.

[20] Cordes, T., Michelucci, A., Hiller, K., 2015. Itaconic acid: the surprising role of an industrial compound as a mammalian antimicrobial metabolite. Annual Review of Nutrition 35:451–473. https://doi.org/10.1146/annurev-nutr-071714-034243.

[21] Chen, F., Lukat, P., Iqbal, A.A., Saile, K., Kaever, V., van den Heuvel, J., et al., 2019. Crystal structure of cis-aconitate decarboxylase reveals the impact of naturally occurring human mutations on itaconate synthesis. Proceedings of the National Academy of Sciences of the United States of America, 201908770. https://doi.org/10.1073/pnas.1908770116.

[22] Seim, G.L., Britt, E.C., John, S.V., Yeo, F.J., Johnson, A.R., Eisenstein, R.S., et al., 2019. Two-stage metabolic remodelling in macrophages in response to lipopolysaccharide and interferon-γ stimulation. Nature Metabolism 1(7):731–742. https://doi.org/10.1038/s42255-019-0083-2.

[23] Meiser, J., Kraemer, L., Jaeger, C., Madry, H., Link, A., Lepper, P.M., et al., 2018. Itaconic acid indicates cellular but not systemic immune system activation. Oncotarget 9(63):32098–32107. https://doi.org/10.18632/oncotarget.25956.

[24] Mills, E.L., Ryan, D.G., Prag, H.A., Dikovskaya, D., Menon, D., Zaslona, Z., et al., 2018. Itaconate is an anti-inflammatory metabolite that activates Nrf2 via alkylation of KEAP1. Nature 556(7699):113–117. https://doi.org/10.1038/nature25986.

[25] Bambouskova, M., Gorvel, L., Lampropoulou, V., Sergushichev, A., Loginicheva, E., Johnson, K., et al., 2018. Electrophilic properties of itaconate and derivatives regulate the IκBζ–ATF3 inflammatory axis. Nature 556(7702): 501–504. https://doi.org/10.1038/s41586-018-0052-z.

[26] Thompson, J.W., Narayanan, S.V., Koronowski, K.B., Morris-Blanco, K., Dave, K.R., Perez-Pinzon, M.A., 2014. Signaling pathways leading to ischemic mitochondrial neuroprotection. Journal of Bioenergetics and Biomembranes. https://doi.org/10.1007/s10863-014-9574-8.

[27] Shih, A.Y., 2005. A small-molecule-inducible Nrf2-mediated antioxidant response provides effective prophylaxis against cerebral ischemia in vivo. Journal of Neuroscience. https://doi.org/10.1523/JNEUROSCI.4014-05.2005.

[28] Sheng, H., Laskowitz, D.T., Mackensen, G.B., Kudo, M., Pearlstein, R.D., Warner, D.S., 1999. Apolipoprotein E deficiency worsens outcome from global cerebral ischemia in the mouse. Stroke 30(5):1118–1124.

[29] Kooy, N.W., Royall, J.A., Ischiropoulos, H., Beckman, J.S., 1994. Peroxynitrite-mediated oxidation of dihydrorhodamine 123. Free Radical Biology & Medicine 16(2):149–156.

[30] Kushnareva, Y.E., Wiley, S.E., Ward, M.W., Andreyev, A.Y., Murphy, A.N., 2005. Excitotoxic injury to mitochondria isolated from cultured neurons. Journal of Biological Chemistry 280(32):28894–28902. https://doi.org/10.1074/jbc.M503090200.

[31] Divakaruni, A.S., Wallace, M., Buren, C., Martyniuk, K., Andreyev, A.Y., Li, E., et al., 2017. Inhibition of the mitochondrial pyruvate carrier protects from excitotoxic neuronal death. The Journal of Cell Biology 216(4):1091–1105. https://doi.org/10.1083/jcb.201612067.

[32] Kim, H.J., Magrané, J., 2011. Isolation and culture of neurons and astrocytes from the mouse brain cortex. Methods in Molecular Biology (Clifton, N.J.) 793: 63–75.

[33] Young, J.D., 2014. INCA: a computational platform for isotopically non-stationary metabolic flux analysis. Bioinformatics (Oxford, England) 30(9): 1333–1335. https://doi.org/10.1093/bioinformatics/btu015.

[34] Cordes, T., Metallo, C.M., 2019. Quantifying intermediary metabolism and lipogenesis in cultured mammalian cells using stable isotope tracing and mass spectrometry. Methods in Molecular Biology (Clifton, N.J.) 1978:219–241.

[35] Divakaruni, A.S., Rogers, G.W., Murphy, A.N., 2014. Measuring mitochondrial function in permeabilized cells using the Seahorse XF analyzer or a clark-type oxygen electrode. Current Protocols in Toxicology/Editorial Board 60:25.2.1–25.2.16. https://doi.org/10.1002/0471140856.tx2502s60.

[36] Shen, H., Campanello, G.C., Flicker, D., Grabarek, Z., Hu, J., Luo, C., et al., 2017. The human knockout gene CLYBL connects itaconate to vitamin B 12. Cell 171(4):771–782. https://doi.org/10.1016/j.cell.2017.09.051 e11.

[37] Murakami, S., Motohashi, H., 2015. Roles of Nrf2 in cell proliferation and differentiation. Free Radical Biology and Medicine 88(Pt B):168–178. https://doi.org/10.1016/j.freeradbiomed.2015.06.030.

[38] Zhao, D., Badur, M.G., Luebeck, J., Magaña, J.H., Birmingham, A., Sasik, R., et al., 2018. Combinatorial CRISPR-cas9 metabolic screens reveal critical redox control points dependent on the KEAP1-NRF2 regulatory Axis. Molecular Cell 69(4):699–708. https://doi.org/10.1016/j.molcel.2018.01.017 e7.

[39] Sayin, V.I., LeBoeuf, S.E., Singh, S.X., Davidson, S.M., Biancur, D., Guzelhan, B.S., et al., 2017. Activation of the NRF2 antioxidant program generates an imbalance in central carbon metabolism in cancer. ELife 6. https://doi.org/10.7554/eLife.28083.

[40] Muir, A., Danai, L.V., Gui, D.Y., Waingarten, C.Y., Lewis, C.A., Vander Heiden, M.G., 2017. Environmental cystine drives glutamine anaplerosis and sensitizes cancer cells to glutaminase inhibition. ELife 6. https://doi.org/10.7554/eLife.27713.

[41] Mitsuishi, Y., Taguchi, K., Kawatani, Y., Shibata, T., Nukiwa, T., Aburatani, H., et al., 2012. Nrf2 redirects glucose and glutamine into anabolic pathways in metabolic reprogramming. Cancer Cell 22(1):66–79. https://doi.org/10.1016/j.ccr.2012.05.016.

[42] Ashrafian, H., Czibik, G., Bellahcene, M., Aksentijević, D., Smith, A.C., Mitchell, S.J., et al., 2012. Fumarate is cardioprotective via activation of the Nrf2 antioxidant pathway. Cell Metabolism 15(3):361–371. https://doi.org/10.1016/j.cmet.2012.01.017.

[43] Acosta, S., Nilsson, T., 2012. Current status on plasma biomarkers for acute mesenteric ischemia. Journal of Thrombosis and Thrombolysis 33(4):355–361. https://doi.org/10.1007/s11239-011-0660-z.

[44] Dorsch, N.W.C., 2002. Therapeutic approaches to vasospasm in subarachnoid hemorrhage. Current Opinion in Critical Care 8(2):128–133.

[45] Mindea, S.A., Yang, B.P., Bendok, B.R., Miller, J.W., Batjer, H.H., 2006. Endovascular treatment strategies for cerebral vasospasm. Neurosurgical Focus 21(3):E13.

[46] Griffin, G.K., Newton, G., Tarrio, M.L., Bu, D. -x., Maganto-Garcia, E., Azcutia, V., et al., 2012. IL-17 and TNF- sustain neutrophil recruitment during inflammation through synergistic effects on endothelial activation. The Journal of Immunology 188(12):6287–6299. https://doi.org/10.4049/jimmunol.1200385.

[47] Murphy, M.P., 2009. How mitochondria produce reactive oxygen species. Biochemical Journal 417(1):1–13. https://doi.org/10.1042/BJ20081386.

[48] Murphy, E., Steenbergen, C., 2008. Mechanisms underlying acute protection from cardiac ischemia-reperfusion injury. Physiological Reviews 88(2):581–609. https://doi.org/10.1152/physrev.00024.2007.

[49] Zweier, J.L., Flaherty, J.T., Weisfeldt, M.L., 1987. Direct measurement of free radical generation following reperfusion of ischemic myocardium. Proceedings of the National Academy of Sciences of the United States of America 84(5): 1404–1407. https://doi.org/10.1073/pnas.84.5.1404.

[50] Abramov, A.Y., Scorziello, A., Duchen, M.R., 2007. Three distinct mechanisms generate oxygen free radicals in neurons and contribute to cell death during anoxia and reoxygenation. Journal of Neuroscience: The Official Journal of the Society for Neuroscience 27(5):1129–1138. https://doi.org/10.1523/JNEUROSCI.4468-06.2007.

[51] Burwell, L.S., Brookes, P.S., 2008. Mitochondria as a target for the cardioprotective effects of nitric oxide in ischemia–reperfusion injury.

Antioxidants and Redox Signaling 10(3):579–600. https://doi.org/10.1089/ars.2007.1845.

[52] Kohlhauer, M., Pell, V.R., Burger, N., Spiroski, A.M., Gruszczyk, A., Mulvey, J.F., et al., 2019. Protection against cardiac ischemia-reperfusion injury by hypothermia and by inhibition of succinate accumulation and oxidation is additive. Basic Research in Cardiology 114(3):18. https://doi.org/10.1007/s00395-019-0727-0.

[53] Valls-Lacalle, L., Barba, I., Miró-Casas, E., Alburquerque-Béjar, J.J., Ruiz-Meana, M., Fuertes-Agudo, M., et al., 2016. Succinate dehydrogenase inhibition with malonate during reperfusion reduces infarct size by preventing mitochondrial permeability transition. Cardiovascular Research 109(3):374–384. https://doi.org/10.1093/cvr/cvv279.

[54] Wojtovich, A.P., Brookes, P.S., 2009. The complex II inhibitor atpenin A5 protects against cardiac ischemia-reperfusion injury via activation of mitochondrial KATP channels. Basic Research in Cardiology 104(2):121–129. https://doi.org/10.1007/s00395-009-0001-y.

[55] Romero, R., Sayin, V.I., Davidson, S.M., Bauer, M.R., Singh, S.X., LeBoeuf, S.E., et al., 2017. Keap1 loss promotes Kras-driven lung cancer and results in dependence on glutaminolysis. Nature Medicine 23(11):1362. https://doi.org/10.1038/nm.4407.

[56] Thimmulappa, R.K., Lee, H., Rangasamy, T., Reddy, S.P., Yamamoto, M., Kensler, T.W., et al., 2006. Nrf2 is a critical regulator of the innate immune response and survival during experimental sepsis. Journal of Clinical Investigation 116(4):984–995. https://doi.org/10.1172/JCI25790.

[57] Sims, C.A., Wattanasirichaigoon, S., Menconi, M.J., Ajami, A.M., Fink, M.P., 2001. Ringer's ethyl pyruvate solution ameliorates ischemia/reperfusion-induced intestinal mucosal injury in rats. Critical Care Medicine 29(8):1513–1518.

[58] Adler, J., Wang, S.-F.F., Lardy, H.A., 1957. The metabolism of itaconic acid by liver mitochondria. Journal of Biological Chemistry 229(2):865–879.

[59] Emmrich, R., 1939. Stoffwechselversuche mit einigen methylierten niedermolekularen Dicarbonsäuren. Hoppe-Seyler´s Zeitschrift Für Physiologische Chemie.

[60] Booth, A.N., Taylor, J., Wilson, R.H., Deeds, F., 1952. The inhibitory effects of itaconic acid in vitro and in vivo. Journal of Biological Chemistry 195(2):697–702.

[61] Eastridge, B.J., Mabry, R.L., Seguin, P., Cantrell, J., Tops, T., Uribe, P., et al., 2012. Death on the battlefield (2001–2011). Journal of Trauma and Acute Care Surgery 73(6 Suppl 5):S431–S437. https://doi.org/10.1097/TA.0b013e3182755dcc.

[62] Sun, X., Zhang, B., Pan, X., Huang, H., Xie, Z., Ma, Y., et al., 2019. Octyl-itaconate inhibits osteoclastogenesis by suppressing Hrd1 and activating Nrf2 signaling. The FASEB Journal: Official Publication of the Federation of American Societies for Experimental Biology. https://doi.org/10.1096/fj.201900887RR fj201900887RR.

[63] Selak, M.a., Armour, S.M., MacKenzie, E.D., Boulahbel, H., Watson, D.G., Mansfield, K.D., et al., 2005. Succinate links TCA cycle dysfunction to oncogenesis by inhibiting HIF-alpha prolyl hydroxylase. Cancer Cell 7(1):77–85. https://doi.org/10.1016/j.ccr.2004.11.022.

[64] Lussey-Lepoutre, C., Hollinshead, K.E.R., Ludwig, C., Menara, M., Morin, A., Castro-Vega, L.J., et al., 2015. Loss of succinate dehydrogenase activity results in dependency on pyruvate carboxylation for cellular anabolism. Nature Communications 6. https://doi.org/10.1038/ncomms9784.

[65] Browne, S.E., Bowling, A.C., MacGarvey, U., Baik, M.J., Berger, S.C., Muqit, M.M.K., et al., 1997. Oxidative damage and metabolic dysfunction in huntington's disease: selective vulnerability of the basal ganglia. Annals of Neurology 41(5):646–653. https://doi.org/10.1002/ana.410410514.

[66] Mills, E.L., Kelly, B., Logan, A., Costa, A.S.H., Varma, M., Bryant, C.E., et al., 2016. Succinate dehydrogenase supports metabolic repurposing of mitochondria to drive inflammatory macrophages. Cell 167(2):457–470. https://doi.org/10.1016/j.cell.2016.08.064 e13.

[67] Németh, B., Doczi, J., Csete, D., Kacso, G., Ravasz, D., Adams, D., et al., 2016. Abolition of mitochondrial substrate-level phosphorylation by itaconic acid produced by LPS-induced Irg1 expression in cells of murine macrophage lineage. The FASEB Journal: Official Publication of the Federation of American Societies for Experimental Biology 30(1):286–300. https://doi.org/10.1096/fj.15-279398.

